Membrane filtration of wastewater effluents for reuse: effluent organic matter rejection and fouling

C. Jarusutthirak and G. Amy

Civil and Environmental Engineering, University of Colorado at Boulder, Boulder, CO 80309, USA

Abstract The reuse of treated wastewater to augment natural drinking water supplies is receiving serious consideration. Treatment of secondary and tertiary effluent by membrane filtration was investigated by assessing nanofiltration (NF) membrane and ultrafiltration (UF) membranes in bench-scale experiments. It was found that secondary and tertiary effluent contained high concentration of effluent organic matter (EfOM), contributing EfOM-related fouling. Flux decline and EfOM rejection tests were evaluated, using a dead-end stirred cell filtration unit. Surface charge and molecular weight cut-off (MWCO) of membranes were significant factors in membrane performance including permeability and EfOM-rejection.

Keywords Effluent organic matter; membranes; wastewater

Introduction

Reclamation of wastewater to augment natural drinking water supplies is receiving increased attention due to the limitation of fresh waters and the increase of water demand. Water quality requirements are specified for each wastewater reuse application (Cole *et al*., 1998). In the USA, federal water pollution control regulations require a minimum of secondary treatment to meet municipal effluent standards; tertiary and/or advanced treatments are needed to achieve higher quality treated waters for reuse.

Membrane filtration has been found to be a successful advanced technology in removal of dissolved organic compounds. The application of membrane filtration to reuse of municipal wastewater effluent will steadily increase with more stringent discharge regulations and supply limitations (Reith and Birkenhead, 1998; Tchobanoglous *et al*., 1998). However, membranes can be easily fouled by effluent organic matter (EfOM) present at high levels in wastewater. EfOM-fouling, defined as the accumulation and/or adsorption of organic materials on the surface, or in the pores of a membrane, affects membrane performance including permeability and EfOM rejection (Speth *et al*., 1998).

In this research, the effects of EfOM-fouling on permeate flux and EfOM-rejection of nanofiltration (NF) and ultrafiltration (UF) membranes is investigated using different source waters including secondary effluent, tertiary effluent, and soiled aquifer treatment (SAT) treated water. Moreover, DOC fractions of feed waters have been analyzed using XAD-8/-4 resins; and the functional groups of EfOM foulants are studied using attenuated total reflection-Fourier transform infrared spectroscopy (ATR-FTIR). The results of this study may help in understanding membrane fouling, leading to the development of pretreatment and cleaning alternatives to control EfOM fouling, and achieving higher performance in membrane filtration.

Source waters and membranes

Three different wastewater effluents, including Boulder (Colorado) secondary effluent (BO-SE), Mesa (Arizona) tertiary effluent (ME-TE), and soil aquifer treatment (SAT) treated water (SAT-TW) were used in membrane fouling experiments. Secondary and tertiary effluents used in these experiments were derived from activated sludge and granular

Water Science and Technology **Vol 43 No10 pp 225–232**

media filtration processes, respectively. SAT-TW was collected from groundwater wells, located down gradient from recharge basins infiltrating reclaimed wastewater.

All water samples were 0.45 μm filtered and stored at 4°C until analysis. Each sample was analyzed for dissolved organic carbon (DOC), UV absorbance at 254 nm (UVA_{254}), specific UVA (SUVA), and DOC-fractionation by XAD-8/-4 resins. Table 1 shows the characteristics of water samples. SUVA is a ratio of UVA_{254} and DOC, indicating an aromatic charater of EfOM. SUVA values were found to be correlated to the humic fraction estimated from XAD-8 resin adsorption (Figure 1).

One nanofiltration (NF) membrane (ESNA) and three ultrafiltration (UF) membranes (GM, PM10, and NTR7410) were employed in the experiments. Each membrane showed different characteristics, resulting in adsorption of different fouling materials, and membrane performances. The ESNA and GM membranes are considered, based on their nominal molecular weight cut-offs (MWCO), as NF and UF membranes, respectively. They are both made of polyamide (PA). The PM10 and NTR7410 membranes, considered as UF membranes, are made of polyethersulfone (PES) and sulfonated PES, respectively (Cho, 1998). The characteristics of different membranes are summarized in Table 2. Contact angle measurements characterize the hydrophobicity of membrane surfaces (Cho, 1998). The greater the contact angle, the larger the hydrophobicity. The ESNA and PM10 membranes show relatively large hydrophobicity. Zeta potential is used to determine the charge on membrane surface. Surface charges of membranes help to determine electrostatic interaction between membranes and solutes/foulants (Cho, 1998). According to Table 2, all tested membranes are shown to be negatively charged membranes; the GM and NTR7410 membranes are found to be highly (negatively) charged membranes in terms of zeta potential.

Methods and analyses

The membrane fouling experiments were conducted using a dead-end stirred cell filtration unit. Both flux-decline and EfOM dynamic adsorption tests were performed to determine

Table 1 Characteristics of source-water samples

Source water	DOC ($mg\ L^{-1}$)	UVA_{254} (cm^{-1})	SUVA ($m^{-1}mg^{-1}L$)	Humic fraction (% DOC)	pH	Conductivity (μS/cm)
BO-SE	7.1	0.135	1.9	41	7.04	697
ME-TE	5.6	0.087	1.6	31	8.34	1430
SAT-TW	1.3	0.031	2.5	38	8.53	1312

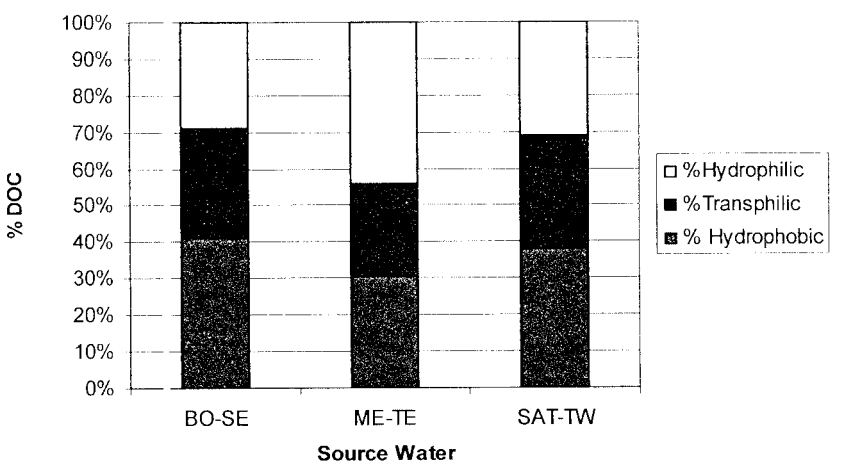

Figure 1 EfOM fractionation of different source waters

Table 2 Characteristics of membranes

Code	Type	Material	MWCO (Dalton)	Contact angle (°)	Zeta potential at pH 7 (mV)	PWP* ($L.day^{-1}.m^2.kPa$)
ESNA	NF	PA	200	60.3	–11.5	1.35
GM	UF	PA	8,000	45.5	–17.0	2.96
PM10	UF	PES	10,000	55.1	–12.8	25.32
NTR7410	UF	sulfonated PES	20,000	49.5	–22.6	4.86

* Pure water permeability

flux-decline trends, EfOM-rejection trends, and EfOM-adsorption trends for different combinations of source waters and membranes.

Flux decline experiments took the form of stirred cell tests with disk membrane specimen tests in a dead-end mode. For flux-decline tests, a 4 litre feed reservoir was employed to provide a continuous supply of feed water, with pressure applied to the reservoir. The transmembrane pressure and initial water flux were recorded. The permeate flux was monitored as a function of volume, time, as well as cumulative delivered (mass-flux) and deposited (adsorbed) DOC. Permeate samples were analyzed for DOC and UVA_{254} using a total organic carbon analyzer (TOC-5000, Shimadzu) and a UV-visible spectrophotometer (UV160A, Shimadzu), respectively. EfOM rejection, delivered DOC, and deposited DOC were then estimated.

For EfOM-dynamic adsorption tests, a water sample of 100 mL was put into the dead-end stirred cell filtration unit. After applying pressure, the sample was passed through the membrane. Permeate and retentate volumes of 50 mL each were collected and the DOC and UVA_{254} of feed water, permeate, and retentate were measured. A mass balance based on DOC was calculated; and the DOC adsorbed on membrane surface, or in membrane pores, were then estimated. Clean and fouled membranes were analyzed by attenuated total reflection-Fourier transform infrared spectroscopy (ATR-FTIR) to determine functional groups associated with membrane surface materials and foulants (Cho, 1998).

Results and discussion

Flux decline and EfOM-dynamic adsorption tests. Flux decline of Boulder-secondary effluent were investigated using four different membranes, including ESNA, GM, PM10, and NTR7410. It was observed that the permeate flux decreased over time and total permeate volume, as shown in Figure 2 and 3, respectively. According to the results, the ESNA membrane exhibited the largest flux decline in comparison to the others. The percentage of flux decline was found to be 80, 35, 58, and 42% for the ESNA, GM, PM10, and NTR7410 membranes, respectively. The decrease of permeate flux was found to be dependent upon EfOM-fouling, occurring by the accumulation of organic materials on membrane surfaces and/or within membrane pores. As EfOM molecules deposited on and/or within membranes, they reduce the permeation rate of the membrane by cake formation, pore blockage, and adsorptive fouling. Those processes are dependent on the characteristics of both membranes and foulants (Wiesner *et al*., 1996).

The effective pore size and surface charge of membranes are considered to be significant factors contributing to the reduction of permeate flux (Schafer *et al*., 1998). The effective pore size of a membrane is a membrane resistance affecting the decrease of permeate flux. The lower the MWCO, the larger the membrane resistance. Negatively charged functional groups associated with EfOM may be electrostatically repulsed by a negatively charged membrane. The more negatively charge density on the membrane surface is correlated to

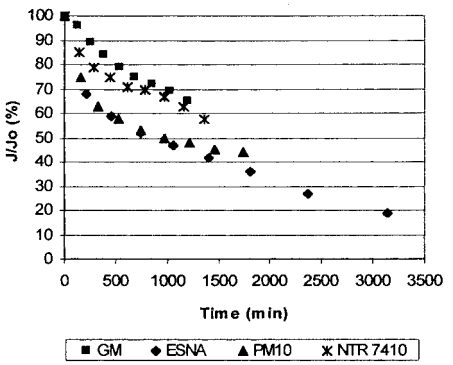

Figure 2 Flux-decline trends of various membranes based on time, using BO-SE

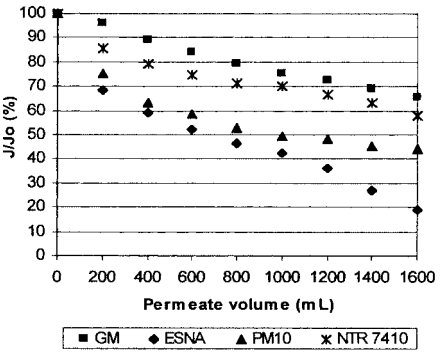

Figure 3 Flux-decline trends of various membranes based on permeate volume, using BO-SE

the greater hydrophilicity of the membrane. As a result, a less negatively surface charge (more hydrophobic) may increase the deposition of hydrophobic EfOM, leading to more adsorptive fouling. Cake resistance provides a significant effect on flux decline. The cake itself may act as a filter and remove smaller particles. Cake formation, pore blockage, and adsorptive fouling may result in resistances to permeate flux that ultimately surpass the membrane resistance (Wiesner *et al*., 1996; Schafer *et al*., 1998; AWWA, 1998).

According to the experiments, the ESNA membrane, representing a low MWCO and less negatively charge, shows a high flux decline trend. This indicates the effect of size exclusion and the accumulation of organic matter on, and/or within, the membrane due to the hydrophobic interaction between EfOM-foulants and the membrane surface. Although the surface charge of the PM10 membrane is similar to that of the ESNA membrane, flux decline exhibited by the PM10 membrane is lower than that by the ESNA membrane. The effect of size exclusion, or steric effects, can be used to explain this phenomenon. The decrease in permeate flux for the GM and NTR7410 membranes was found to be smaller than the others due to a combination of charge interaction and size exclusion (Yoon , 1998).

The decrease in permeate flux reflects the increase in the mass of EfOM deposited on the membrane. When cake resistance and adsorptive fouling are high relative to the resistance of the membrane, flux decline may be correlated with the mass of deposited materials on and/or in membrane. Figures 4 and 5 show the relationship between flux decline and delivered DOC, and rejected DOC, respectively. Permeate flux was shown to decrease as delivered DOC and rejected DOC increase.

The ESNA and GM membranes were used in flux decline tests with two different source waters including Mesa-tertiary effluent (ME-TE), and SAT-treated water (SAT-TW). Figure 6 shows flux decline trends of ME-TE, and SAT-TW, referred to as OW2-90. An OW2 well is located 722 feet down gradient from the recharge basin. The sample from this well contains 90–95 percent reclaimed water. The results show the different flux decline trends of ME-TE and OW2-90. This implies that EfOM-foulants may be reduced by tertiary treatment system. However, relatively high flux reduction by ESNA membranes may be contributed by inorganic fouling. Figure 7 illustrates flux decline trends of ME-TE in comparison to composite SAT-TW collected down gradient from the recharge basin, referred to as SIBW-TW; this test was conducted using the GM membrane. The composite SIBW-TW was collected from different wells located 3,000 to 12,750 feet from the recharge basins, and the average percent reclaimed water was 50 percent approximately. The result shows that ME-TE exhibited higher flux decline than the SIBW-TW. It can be concluded that EfOM present in reclaimed water affected permeate flux. The reduction in permeate flux of SAT-TW is lower than that of ME-TE, indicating that EfOM is removed during transport through the soil.

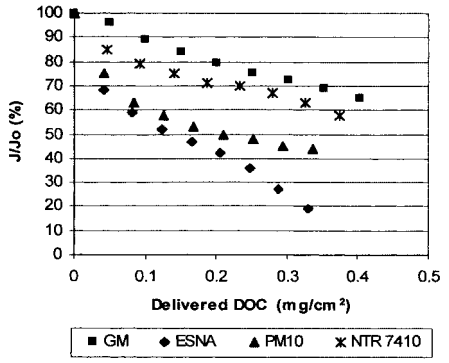

Figure 4 Flux-decline trends of various membranes based on delivered DOC, using BO-SE

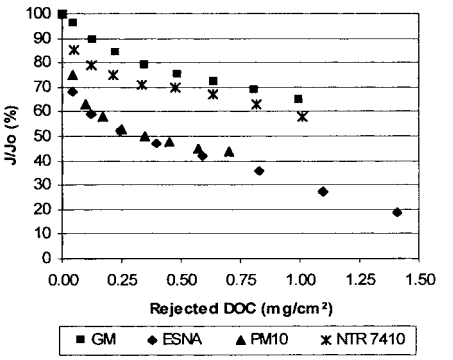

Figure 5 Flux-decline trends of various membranes based on rejected DOC, using BO-SE

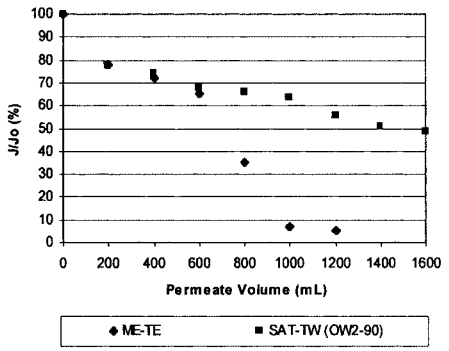

Figure 6 Flux-decline trends of ESNA membranes based on permeate volume using different source waters

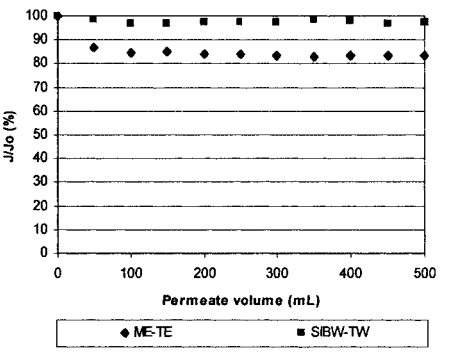

Figure 7 Flux-decline trends of GM membranes based on permeate volume, using different source water

EfOM-dynamic adsorption tests were conducted to determine the adsorbed DOC on and/or in various membranes. It was found that the adsorbed DOC increased with the increase in delivered DOC. Figure 8 illustrates the EfOM adsorption trends with four different membranes as a function of delivered DOC. The results show different trends. Even though the ESNA and PM10 have less negatively surface charges and exhibited higher flux decline, the adsorbed EfOM on ESNA and PM10 membranes was lower than that on GM and NTR7410. This may be explained as a consequence of back transport processes; as the thickness of the cake was higher, back transport became more considerable (Wiesner *et al.*, 1996).

EfOM rejection. EfOM rejection tests were conducted using a dead-end stirred cell filtration unit with four different membranes and BO-SE. Figures 9 and 10 show EfOM rejection trends based on DOC and UVA, respectively, as a function of time. The ESNA membrane provided the greatest DOC rejection (90–92%). The GM and NTR7410 membranes exhibited removal efficiencies of 28–55%, and 37–54%, respectively, which are relatively high for UF membranes. The PM10 membrane exhibited a percent removal of 25–37%. The EfOM rejection based on UVA illustrates similar trends as those based on DOC. The significant mechanisms of EfOM rejection are size exclusion (MWCO) and charge interaction (electrostatic repulsion) (Schafer *et al.*, 1998). The ESNA membrane was found to be very effective in removal of EfOM due to its MWCO and negatively charged surface.

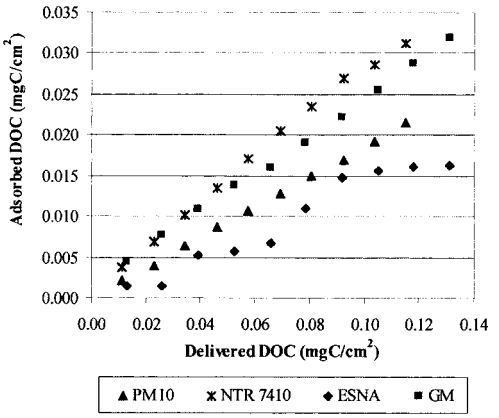

Figure 8 EfOM adsorption trends with PM10, NTR7410, ESNA, and GM membranes

Electrostatic effects were likely dominant in EfOM rejection by the NTR7410 membrane. Even though the NTR7410 membrane had a much larger MWCO than the GM membrane, EfOM rejection by the NTR7410 membrane was observed to be higher than the GM membrane. The greater negative surface charge of the NTR7410 membrane provided higher EfOM rejection. On the other hand, the lesser EfOM rejection shown by the PM10 membrane may be attributed to its less negative surface charge and higher MWCO.

FTIR spectra of clean and fouled membranes. Clean and fouled membrane surfaces were analyzed for functional groups using attenuated total reflection-Fourier transform infrared spectroscopy (ATR-FTIR). The differences in IR spectra between clean and fouled membranes may explain the adsorption phenomena of the foulants onto the membrane surfaces. The peaks at wave numbers of 1540 cm^{-1} and/or 1640 cm^{-1} indicate the functional group of aromatic carbons. The peaks between 1040 and 1240 cm^{-1} show C-O bonds of ethers, carboxylic acids, and polysaccharides (Cho, 1998; Cho *et al*., 1998). Figures 11a–11d illustrate the comparison of IR peaks between clean and fouled membranes of ESNA, GM, PM10, and NTR7410 membranes, respectively. Foulant materials were present in the Boulder-secondary effluent, Mesa-tertiary effluent, and SAT-treated water. When the membranes were fouled with foulants, some of the peaks of clean membranes were changed in absorbance intensity, indicating the functional groups of foulants. The difference in absorbance intensity of IR peaks around 960–1170 cm^{-1} indicates the possibility of

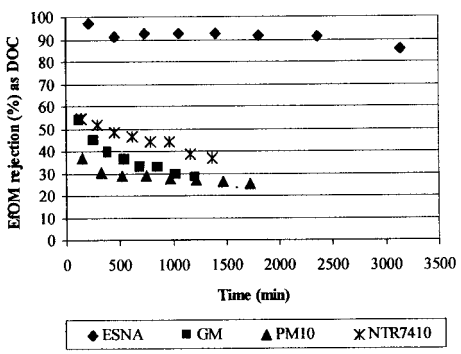

Figure 9 EfOM rejection for BO-SE based on DOC as a function of time

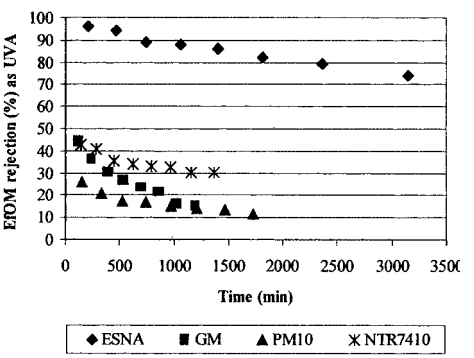

Figure 10 EfOM rejection for BO-SE based on UVA as a function of time

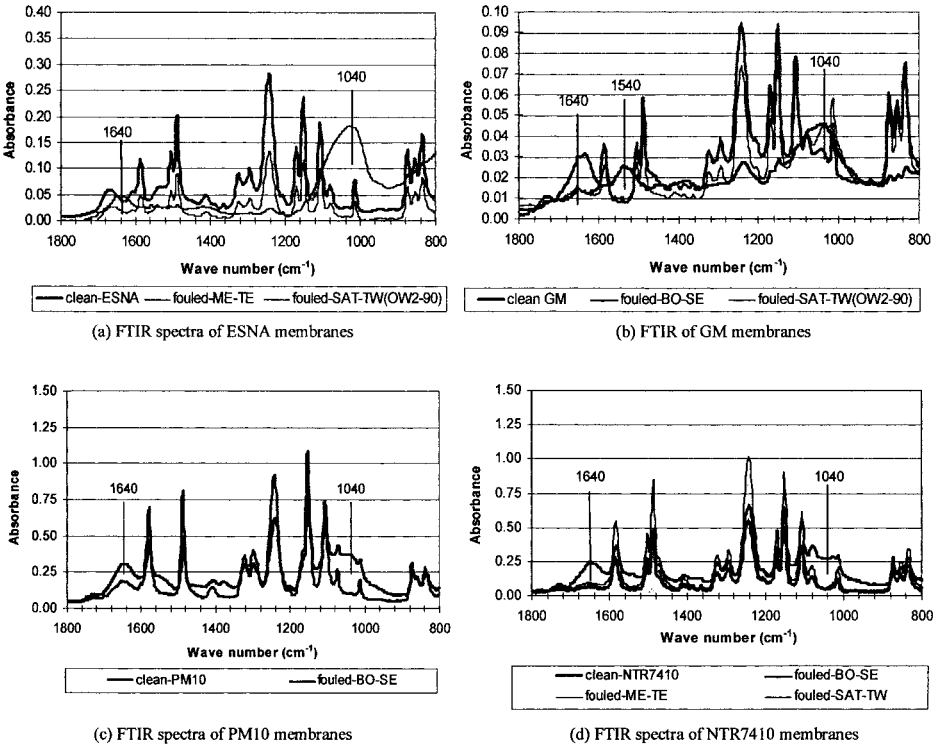

Figure 11 FTIR spectra of clean and fouled membranes with BO-SE, ME-TE, and SAT-TW

polysaccharides or polysaccharide-like substances as foulants. The IR peaks around 1540 cm^{-1} and 1640 cm^{-1} indicate the adsorption of aromatic carbon, possibly containing in hydrophobic portion of EfOM (Cho, 1998; Cho *et al.*, 1998). The IR peaks of Boulder-secondary effluent and Mesa-tertiary effluent were found at 1040, 1540, and 1640 cm^{-1}, indicating the possible foulants as humic fraction, and polysaccharides (Cho, 1998). Those possible foulants were found to be reduced in the SAT-treated water, reflecting the effectiveness of soil aquifer treatment in EfOM removal.

Conclusions

Flux decline, EfOM rejection and fouling mechanisms were dependent on the charge of the membrane surface and the molecular weight cut-off (MWCO). The negatively charged surface led to the adsorption of hydrophobic portion of EfOM. This phenomenon results in a decrease in permeate flux and increase in EfOM rejection. The ESNA membrane was found to be very effective in removal of EfOM, but ineffective in terms of maintaining flux decline. The GM and NTR7410 membranes provided less flux decline than ESNA membrane because of higher negatively charged surfaces. The PM10 membrane exhibited low EfOM rejection but high flux decline because of its low surface charge and high MWCO. The FTIR and EfOM-fractionation data indicated that humic fractions and polysaccharides may be significant foulants in both secondary and tertiary effluent, but not in SAT-treated water. Study of the characteristics of EfOM-foulants as well as the effect of EfOM-fouling on membrane flux decline and EfOM rejection may lead to an improvement of membrane performance in wastewater reuse.

References

AWWA membrane technology research committee (1998). Committee report: membrane processes, *J. AWWA*, **90**, 91–105.

Cho, J. (1998). *Natural organic matter (NOM) rejection by, and flux-decline of, nanofiltration (NF) and ultrafiltration (UF) membranes*. Ph.D. dissertation, Department of Civil, Environmental, and Architectural Engineering, University of Colorado at Boulder.

Cho, J., Amy, G., Pelligrino, J. and Yoon, Y. (1998). Characterization of clean and natural organic matter (NOM) fouled NF and UF membranes, and the foulants characterization, *Desalination*, **118**, 101–108.

Cole, S. (1998). Reclaimed wastewater continues flow toward tap, *Env. Sci. Tech.*, **41**, 496A–497A.

Reith, C. and Birkenhead, B. (1998). Membranes enabling the affordable and cost effective reuse of wastewater as an alternative water source, *Desalination*, **117**, 203–210.

Schafer, A.I., Fane, A.G. and Waite, T.D. (1998). Nanofiltration of natural organic matter: removal, fouling, and the influence of multivalent ions, *Desalination*, **118**, 109–122.

Speth, T.F., Summers, S.R. and Gusses, A.M. (1998). Nanofiltration foulants from a treated surface water, *Envi. Sci. Tech.*, **32**(22), 3612–3617.

Tchobanoglous, G., Darby, J., Bourgeous, K., McArdle, J., Genest, P. and Tylla, M. (1998). Ultrafiltration as an advanced tertiary treatment process for municipal wastewater, *Desalination*, **119**, 315–322.

Wiesner, M.R. and Aptel, P. (1996). Mass transport and permeate flux and fouling in presure driven processes. In: *Water Treatment Membrane Processes*, McGraw-Hill, New York, pp. 4.1–4.30.

Yoon, Y. (1998). *Effects of NOM adsorption and deposition on nanofiltration and ultrafiltration membrane flux and flux decline*. Master thesis, Department of Civil, Environmental, and Architectural Engineering, University of Colorado at Boulder.